Low-Grade Ilmenite Leaching Kinetics Using Hydrochloric Acid: RSM and SCM Approaches

Yayat Iman Supriyatna[1,2*], Agus Prasetya[2], Widi Astuti[1], Slamet Sumardi[1], Priskila Natalia[2], Dicky Marsa Adythia[2], and Himawan Tri Bayu Murti Petrus[2]**

[1]*Research Center for Mining Technology, National Research and Innovation Agency (PRPTB-BRIN), Jl. Ir. Sutami Km. 15, Tanjung Bintang, Lampung Selatan 35361, Indonesia*

[2]*Sustainable Mineral Processing Research Group, Department of Chemical Engineering, Faculty of Engineering, Universitas Gadjah Mada, Jl. Grafika No. 2, Yogyakarta 55281, Indonesia*

* ***Corresponding author:***

email: yayat_iman@yahoo.com; bayupetrus@ugm.ac.id***

Received: November 11, 2022
Accepted: August 14, 2023

DOI: 10.22146/ijc.79092

Abstract: *Minerals containing TiO_2 are common in Indonesia, such as ilmenite in iron sand deposits scattered along the country's coasts. Ilmenite is an important source of titanium. One method for making TiO_2 from ilmenite is by solubilizing both the Fe and Ti elements in HCl and then immediately hydrolyze the Ti. The leaching of low-grade ilmenite (ground to 0.177–0.149 mm) is studied kinetically by HCl in a stirred reactor. The research was conducted using the caustic fusion method followed by HCl leaching. The leaching reaction kinetics at the optimum conditions are analyzed using response surface methodology (RSM) with a second-order polynomial equation model and SSE with the shrinking core model (SCM). The results showed that HCl concentration and leaching time were directly proportional to the leached titanium concentration. In contrast, the leaching temperature was inversely proportional. The optimum operating conditions were obtained at a temperature of 30 °C, 9 M HCl, and 120 min of leaching time. The shrinking core model is a better representation of the kinetics than RSM with a second-order polynomial equation model. Based on SCM, the rate of the leaching reaction of titanium from low-grade ilmenite is controlled by diffusion through the ash layer.*

Keywords: *hydrochloric acid; ilmenite; kinetics; leaching; titanium dioxide*

■ INTRODUCTION

Indonesian ilmenite is found in the form of titan laterite and placer with ore reserves of 412,826,836 tons spread across several regions, including Banten [1]. Global titanium reserves are estimated to be 0.75 million tons (0.70 million tons of ilmenite and 0.05 million tons of rutile). In 2021, global ilmenite and rutile ores production must reach 8,400 and 630 million tons, respectively. The world's ilmenite resources represent around 90% of the world's titanium mineral consumption. The world's anatase, ilmenite, and rutile resources total more than 2 billion tons. There is an expanding market for TiO_2 as a pigment. The production of TiO_2 pigment is ramping up to fulfill the demand, with global production capacity reaching 8.4 million tons in 2021 [2-6]. Titanium metal sponge product has further risen steadily, reaching 350 thousand tons in 2021, up from 341 thousand tons in 2020 [2-6], and is estimated to increase further as the metal's use in aerospace and other industries expands.

High-grade or synthetic rutile feedstock is needed for TiO_2 production through the chloride procedure [7-11]. Ilmenite is generally upgraded to synthetic rutile with more than 85% TiO_2 by leaching out the Fe using hydrochloric acid (HCl) after a pretreatment step (redox reactions) [12-13]. The reactivity of ilmenite differs based on its origin. Some ilmenites are difficult to dissolve in HCl and must first be oxidized and reduced, but a few are moderately dissolvable in HCl immediately [14-18]. Caustic fusion is one alternative method that is more environmentally friendly by using alkalis such as

sodium hydroxide (NaOH) and potassium hydroxide (KOH) followed by acid leaching [19-24].

The direct production of pigment-grade TiO_2 from Fe and Ti-containing ilmenite digestion solution through HCl could be examined. Because the Ti must be dissolvable and its subsequent hydrolysis should actually happen in a precise way (i.e., no major hydrolysis can have apparently happened earlier), the digestion requirements differ from those usually used.

Investigation into the variables (concentrations and temperature) that influence ilmenite solubilization in HCl prevents further leaching and inhibits digestion [25]. The reactivity of Indonesian low-grade ilmenite in concentrated HCl on a specific setting appropriate for industrial TiO_2 manufacturing is explained here. The data are then applied to develop a model of the digestion process.

■ EXPERIMENTAL SECTION

Materials

An ilmenite sample was supplied by Rancecet in Banten, Indonesia. As chemicals, NaOH (99) from Merck, Germany and HCl (37%) from SMART-LAB, Indonesia were utilized.

Instrumentation

The elemental composition of ilmenite sand was determined using X-ray fluorescence (XRF, PANalytical Epsilon3^{XLE}) with an analysis time of 20 min and the compound was determined using X-ray diffraction (XRD, PANalytical X'Pert^3 Powder) with an analysis time of 6 min for Cu radiation in the range of 2θ = 10–80°.

Procedure

Ilmenite sand is sieved using a sieve shaker to obtain sand with a size of 0.177–0.149 mm. The ilmenite (93.6 g) and NaOH (26.3 g) are put into a stainless-steel bowl and then calcined in the furnace. Calcination is carried out at a temperature of 850 °C for 40 min. The calcined frit is taken out from the stainless-steel bowl and then mashed.

The calcined frit is put into a beaker and then 382 mL of aquadest is added. The beaker glass is placed on a magnetic stirrer and then leached for 15 min at a temperature of 75 °C. The stirrer speed is set at 300 rpm. The leaching of HCl was carried out at a constant solid-liquid ratio of 1:5 g/mL and a stirring speed of 300 rpm. The filtrate samples were taken at 1, 10, 30, 60, and 120 min. Acid leaching is carried out at three temperature variations (30, 60, and 90 °C) and three HCl concentration variations (1, 5, and 9 M). The composition of the filtrate is analyzed using inductive coupled plasma (ICP) Plasma Quant 9000 Elite.

■ RESULTS AND DISCUSSION

Raw Material Characterization

The results of the XRF analysis in Table 1 show that iron (Fe) and titanium (Ti) are the major elements that make up the Banten iron sand sample, each of which is 60.813 and 31.841%. In addition, Banten iron sand also contains several elements in small amounts, such as silica (Si), calcium (Ca), manganese (Mn), zircon (Zr), aluminum (Al), phosphate (P), and magnesium (Mg).

To recognize the constituent minerals in iron sand samples, XRD testing was used. Fig. 1 depicts the data of the XRD pattern. The main mineral phases of Banten iron sand, according to the XRD pattern, are ilmenite ($FeTiO_3$), magnetite (Fe_3O_4), and magnesioferrite ($MgFe_2O_4$), where the intensity of these three minerals is the greatest. The element Ti in Banten iron sand is found in the ilmenite phase. The ilmenite content in Banten iron sand is quite dominant which is indicated by its high intensity. Based on XRF analysis data and the assumption that Ti is entirely contained in ilmenite, it can be estimated that the amount of ilmenite in iron sand is 68.98%.

Table 1. Elemental composition of Banten iron sand

Element	Content (%)
Fe	60.813
Ti	31.841
Si	2.304
Ca	1.117
Al	1.168
Mn	1.065
Mg	0.610
P	0.324
Zr	0.249

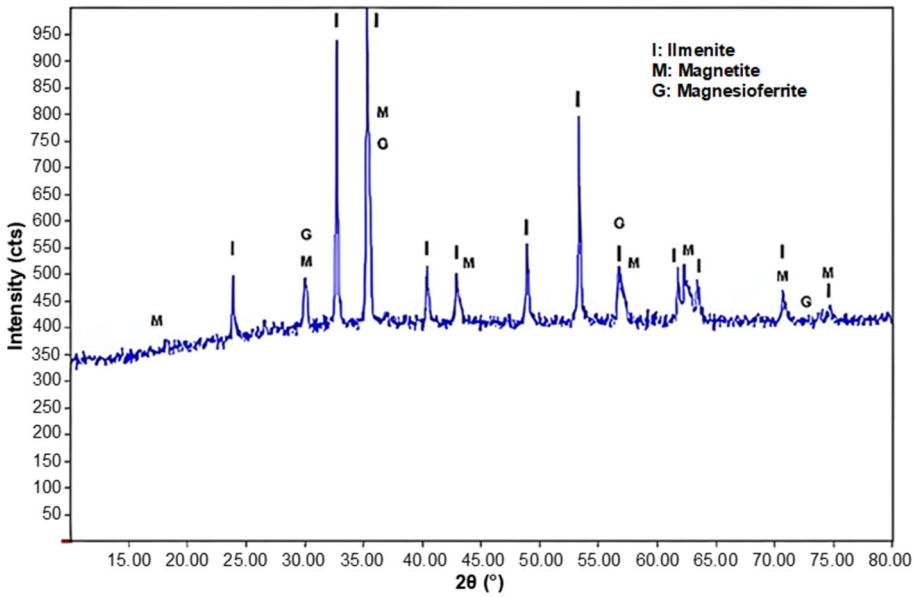

Fig 1. Diffractogram pattern from XRD analysis of Banten ilmenite sample

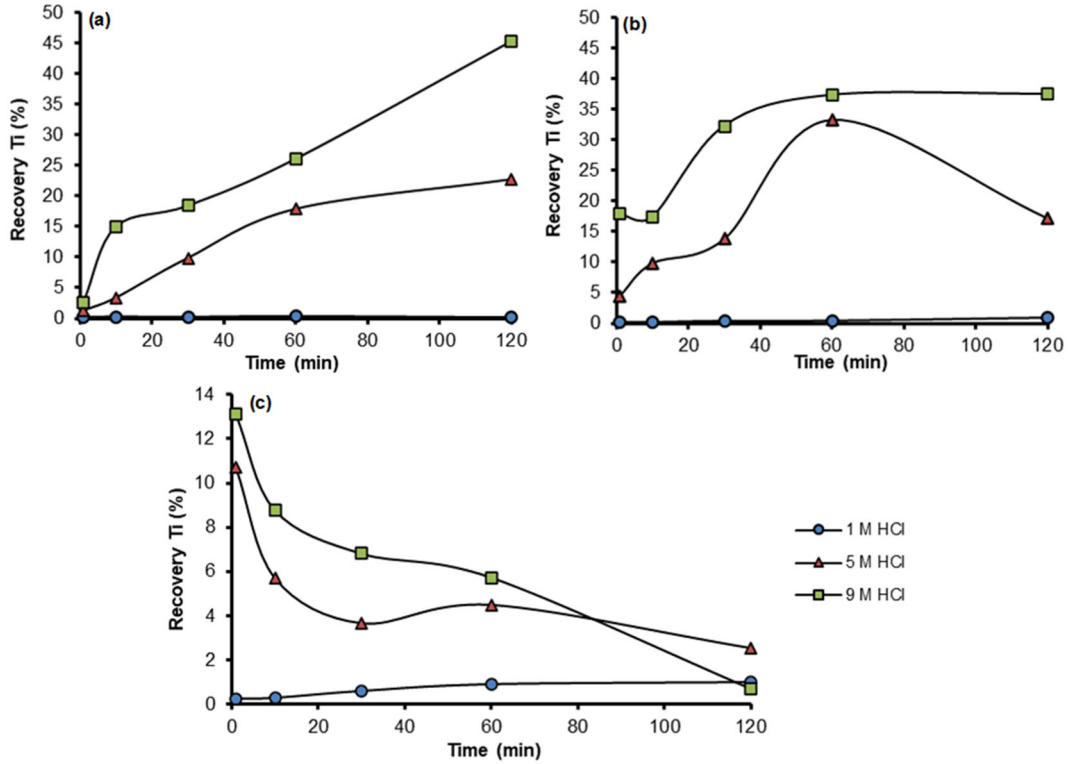

Fig 2. Recovery of titanium at various leaching times and concentrations of HCl at constant temperature (a) 30 °C, (b) 60 °C, and (c) 90 °C

Effect of HCl Concentration

Fig. 2 shows that the higher the HCl concentration used, the higher the recovery value of Ti. It occurs because the higher the HCl concentration used, the more Cl^- ions present in the solvent so that more TiO^{2+} ions bound [12,26].

Effect of Temperature

Fig. 3 indicates that the higher the temperature used, the greater the Ti recovery. This indicates that the Ti leaching process is activated by temperature. The use of higher temperatures will cause high molecular kinetic energy so that intermolecular collisions occur more often, and the stages of product formation will be faster [27].

However, at too high a temperature and HCl concentration, Ti leaching showed different behavior. Fig. 2(b) and 2(c) show that the percent recovery of Ti decreases with increasing temperature. This phenomenon occurs due to the hydrolysis reaction of the product in the form of dissolved titanium ($TiOCl_2$) into metatitanic acid (H_2TiO_3) which is difficult to dissolve in acid as the result of continuous heating [14]. Another possibility is that the heating treatment will cause the hydrolysis speed of Ti to exceed its leaching speed so that the concentration of Ti in the liquid phase will decrease [26,28-29]. The hydrolysis reaction that occurs can be seen in Eq. (1) as follows:

$$TiOCl_2 + 2H_2O \rightarrow H_2TiO_3 + 2HCl \quad (1)$$

Based on the calculation results, the optimum operating conditions for the leaching process of Ti from ilmenite are 9 M of HCl concentration at 30 °C.

Leaching Time

According to Fig. 2 and 3, the longer the leaching time, the higher the concentration of Ti. This is because the solid and liquid phase ions can be in longer contact and more reactions can occur. Unlike the case with the effect of HCl concentration on leached Ti concentrations which continues to increase, the effect of leaching time on leached Ti concentrations will go to an asymptotic point. This is because there will be a significant decrease in leaching reactions after a certain period of time, or in this case when the leaching time exceeds 2 h [12]. Therefore, the variable leaching time must be optimized so that both the process efficiency and the Ti concentration can be maximized.

Leaching Kinetics

Response surface methodology (RSM) analysis

This experiment has 45 combinations of variable operating conditions. The leaching temperature variable

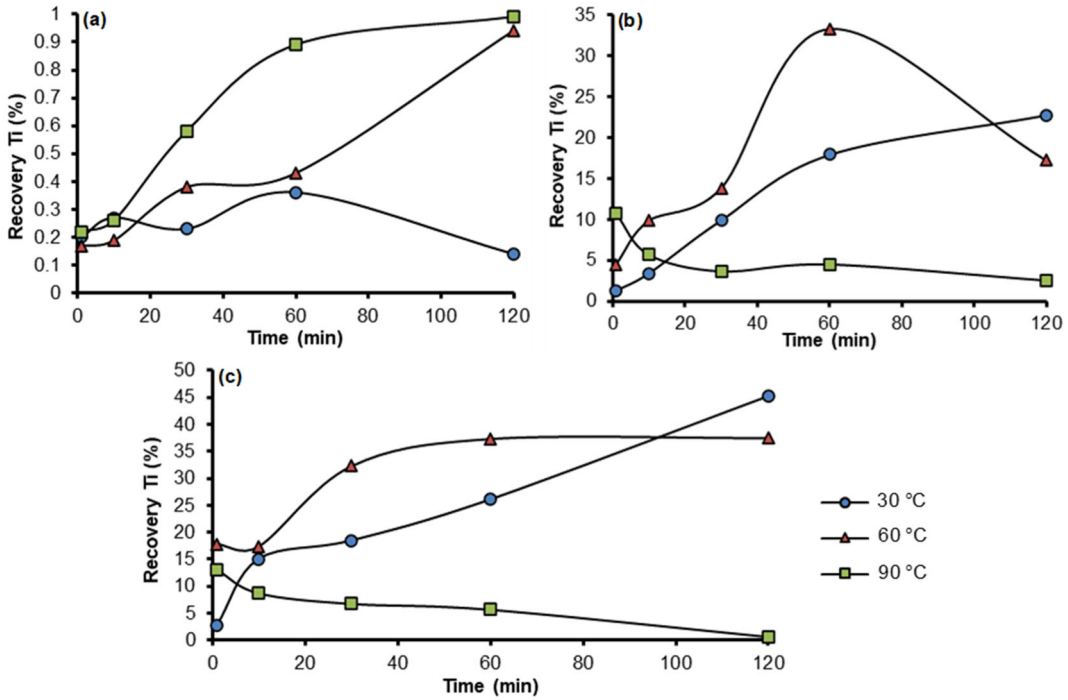

Fig 3. Recovery of titanium at various leaching times and temperatures at constant HCl concentrations (a) 1 M, (b) 5 M, and (c) 9 M

was varied into 30, 60, and 90 °C. The concentration of hydrochloric acid varied into 1, 5, and 9 M. The leaching sampling time was taken at 1, 10, 30, 60, and 120 min. All sample combinations were processed to estimate the coefficient of the regression equation. The equation used is the 2nd order polynomial equation [30]. The regression equation coefficient (Table 2) is obtained through a parameter fitting. The data on the concentration of titanium in this research were used as reference data. The completion of the fitting is done using the 'response surface' tool in Minitab 19 software.

Based on the regression result, the equation will be:

$$y = -26.05 + 0.736x_1 + 2.728x_2 + 0.2364x_3 - 4.95 \times 10^{-3} x_1^2 - 0.0450x_2^2 - 6.96 \times 10^{-4} x_3^2 - 0.0181x_1x_2 \quad (2)$$

Based on the calculation results, the R^2 value for the regression equation was 0.7938, while the adjusted R^2 value was 0.7408. The R^2 value obtained cannot yet approach the value 1. The adjusted R^2 value shows how significant the variables used in the equation model are. The adjusted R^2 value which is below the R^2 value means that there are still less significant variables in the regression equation model. This can also be further clarified using the P-value and the pareto chart. The analysis of variance (ANOVA) table is presented in Table 3, while the Pareto chart is presented in Fig. 4.

According to Craparo [31], the value of significance level or α is generally 5% or 0.05. Predictors in the equation model can be said to have a significant impact on the response variable when the P-value is less than α. Based on the P-value in Table 2, it can be seen that the predictor that has the greatest impact is the x_2 predictor, followed by the predictors x_1x_3, x_1, x_3, x_1^2, x_2x_3, and x_1x_2, respectively. On the other hand, the predictor with the least significant impact was the predictor x_2^2, followed by the predictor x_3^2. The pareto chart in Fig. 4 also gives the same conclusion. The predictor bar that does not cross the reference line means that the predictor is not significant for the response variable [32].

Table 2. Estimated regression equation coefficient

Estimated coefficient	Coefficient
Constant	−26.0500
x_1	0.7360
x_2	2.7280
x_3	0.2364
x_1^2	-4.9500×10^{-3}
x_2^2	−0.0450
x_3^2	-6.9600×10^{-4}
x_1x_2	−0.0181
x_1x_3	-2.5770×10^{-3}
x_2x_3	0.0104

Table 3. Analysis of variance (ANOVA)

Source	Degree of freedom	Sum of square	P-value
Model	9	2389.32	
Linear	3	1864.56	
x_1	1	262.06	0.000
x_2	1	1395.95	0.000
x_3	1	206.55	0.002
Square	3	248.05	
x_1^2	1	198.86	0.002
x_2^2	1	5.17	0.593
x_3^2	1	44.02	0.124
2-way interaction	3	522.94	
x_1x_2	1	94.70	0.027
x_1x_3	1	331.22	0.000
x_2x_3	1	97.02	0.025
Error		620.55	
Total		3009.87	

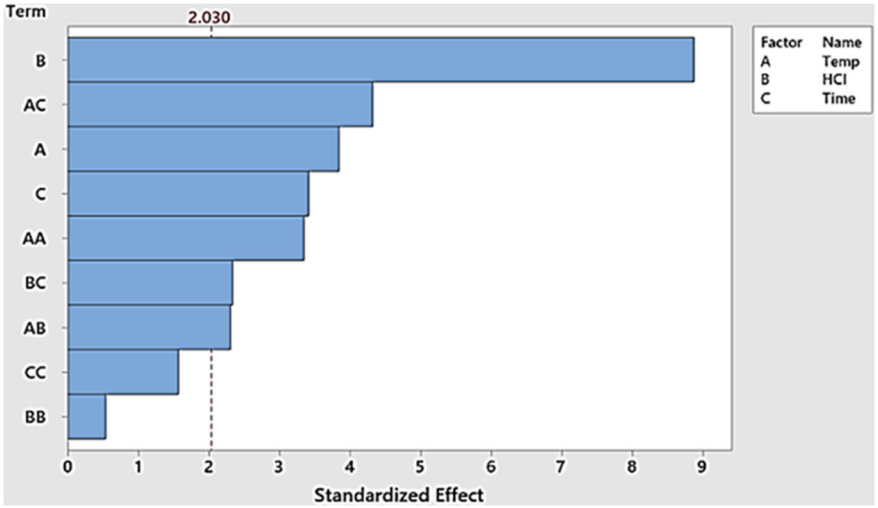

Fig 4. Pareto chart

Based on Table 3 and Fig. 4, it can be concluded that the predictor of the square model does not have a significant impact on the calculation of the response variable.

Shrinking core model (SCM) analysis

The leaching reaction kinetics at the optimum operating conditions is analyzed using the Shrinking Core Model (SCM). The equations obtained (Eq. (2-4)) from the definition of the SCM are as follows [27]:

1st model: diffusion through film layer control: $k_f.t = x$ (2)

2nd model: diffusion through ash layer control: $k_d.t = 1-3(1-x)^{0.67} + 2(1-x)$ (3)

3rd model: chemical reaction control: $k_r.t = 1-(1-x)^{0.33}$ (4)

where x is the fraction mass of the recovered titanium, t is the time, k_f, k_d, and k_r are the reaction rate constants. The results of reaction kinetics simulations are presented in Fig. 5-7. From the simulation results, the

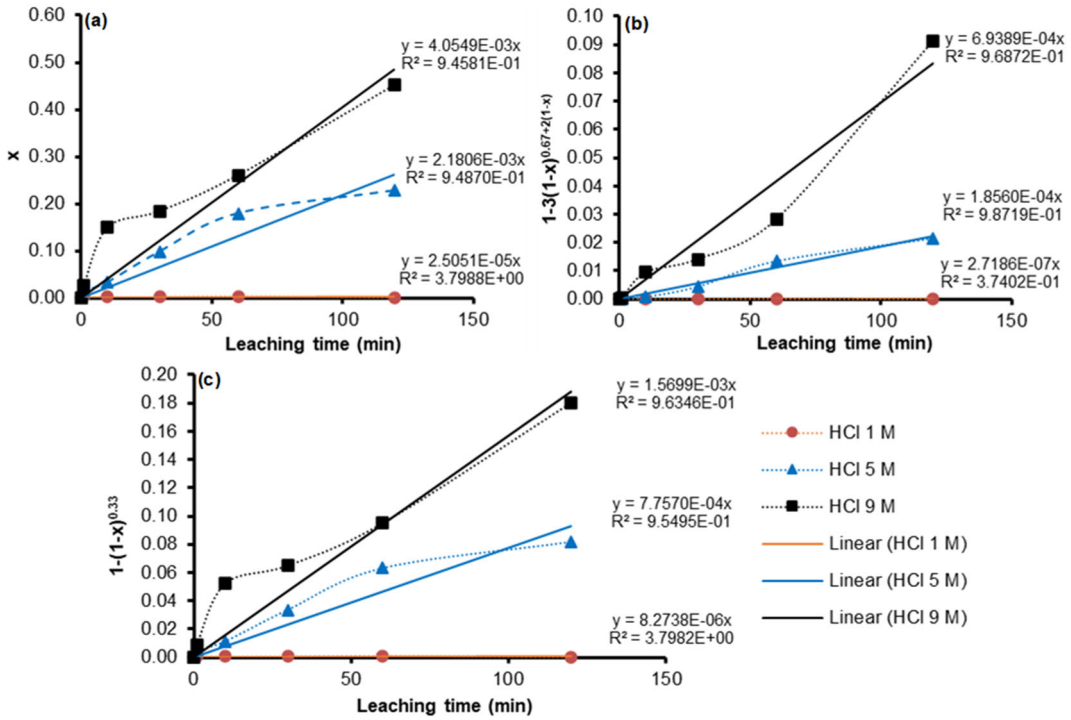

Fig 5. Simulation results using a shrinking core model at 30 °C; (a) diffusion through film layer control, (b) diffusion through ash layer control, and (c) chemical reaction control

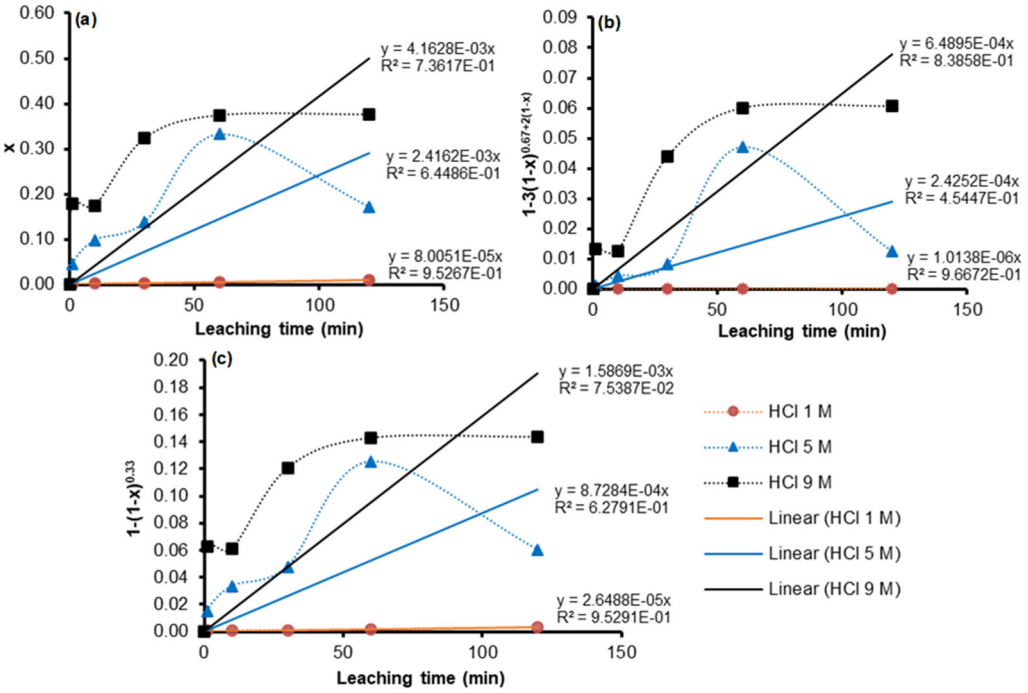

Fig 6. Simulation results using a SCM at 60 °C; (a) diffusion through film layer control, (b) diffusion through ash layer control, and (c) chemical reaction control

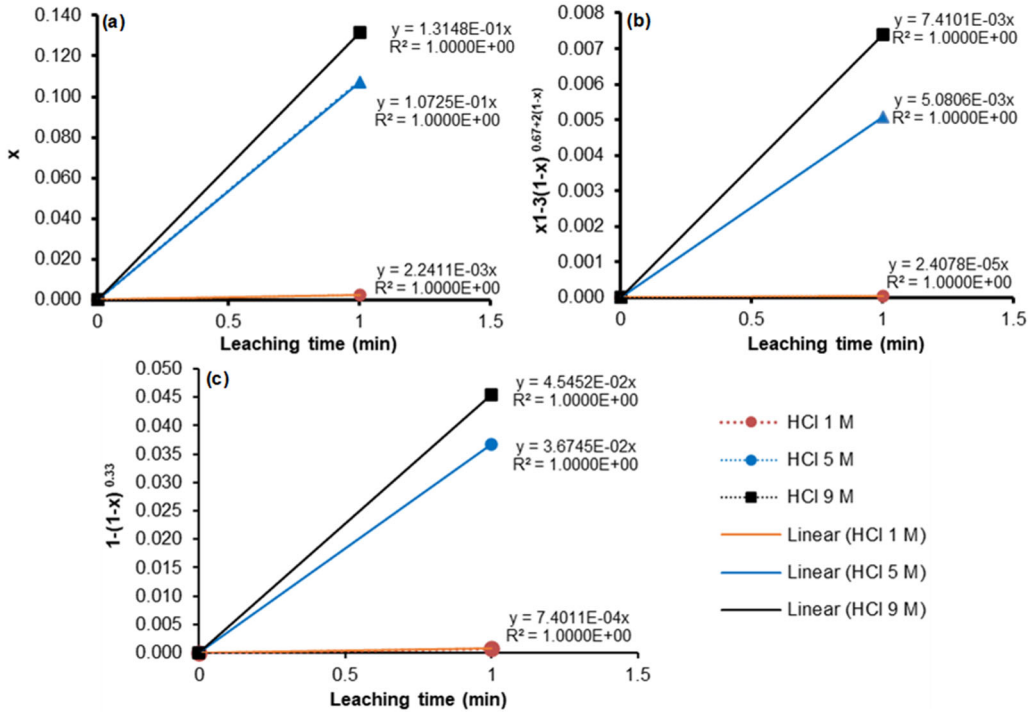

Fig 7. Simulation results using a SCM at 90 °C; (a) diffusion through film layer control, (b) diffusion through ash layer control, and (c) chemical reaction control

reaction rate constants and the sum of squared errors are obtained which are presented in Table 4. Based on kinetic analysis results, the reaction rate constant is directly proportional to the HCl concentration and temperature.

Table 4 shows that the second model gives the smallest SSE value. It indicates that diffusion through the ash layer regulates the rate of Ti leaching from ilmenite. The results obtained are matching with previous research results which state that the mathematical model in which the diffusion stage through the ash layer is the most suitable model for the leaching process [27].

Kinetics calculations at a temperature of 90 °C only use the data from 0 until 1 min because the reaction rate decreases after the first minute. XRF analysis in Fig. 8 shows that with increasing leaching temperature, the Ti content in the leaching residue is higher while the Fe content is lower. It was caused by the hydrolysis reaction of the leaching product in the form of $TiOCl_2$, which was dissolved in the solvent to become a precipitate of H_2TiO_3. The rate of the hydrolysis reaction is affected by the temperature. At temperatures above 90 °C, the hydrolysis reaction rate is greater than the leaching rate, so more Ti is deposited than dissolved. Increasing the concentration of HCl used changes the selectivity of leaching because a lot of Fe is also dissolved, resulting in a lower Fe content in the acid leaching residue [33-34].

Phase Transformation

This investigation also looked at the transformation of the solid phase after the leaching process with the leaching temperature variable varied into 30, 60, and 90 °C and the concentration of HCl was varied into 1, 5, and 9 M.

The XRD analysis of the acid leaching residue in Fig. 9 revealed that the peaks formed were nearly identical. The XRD analysis revealed that the diffractograms produced by the same concentration of HCl solution were nearly identical (RPIB 1P=RPIB

Table 4. Calculation results of reaction rate constants

T (°C)	C_{HCl} (M)	Reaction rate constant (min^{-1})			SSE		
		k_f	k_d	k_r	1st model	2nd model	3rd model
30	1	2.51×10^{-5}	2.72×10^{-7}	8.27×10^{-6}	1.95×10^{-5}	1.89×10^{-5}	1.95×10^{-5}
	5	2.18×10^{-3}	1.86×10^{-4}	7.76×10^{-4}	4.89×10^{-3}	1.19×10^{-3}	3.99×10^{-3}
	9	4.05×10^{-3}	6.94×10^{-4}	1.57×10^{-3}	1.79×10^{-2}	4.41×10^{-1}	1.39×10^{-2}
60	1	8.01×10^{-5}	1.01×10^{-6}	2.65×10^{-5}	6.05×10^{-6}	5.16×10^{-6}	6.05×10^{-6}
	5	2.42×10^{-3}	2.43×10^{-4}	8.73×10^{-4}	6.11×10^{-2}	3.17×10^{-2}	5.71×10^{-2}
	9	4.16×10^{-3}	6.49×10^{-4}	1.59×10^{-3}	1.18×10^{-1}	4.25×10^{-2}	1.03×10^{-1}
90	1	2.24×10^{-3}	2.41×10^{-5}	7.40×10^{-4}	2.38×10^{-16}	3.12×10^{-16}	5.02×10^{-10}
	5	1.07×10^{-1}	5.08×10^{-3}	3.67×10^{-2}	1.20×10^{-11}	4.81×10^{-14}	1.03×10^{-6}
	9	1.31×10^{-1}	7.41×10^{-3}	4.55×10^{-2}	3.08×10^{-12}	1.32×10^{-15}	1.50×10^{-6}

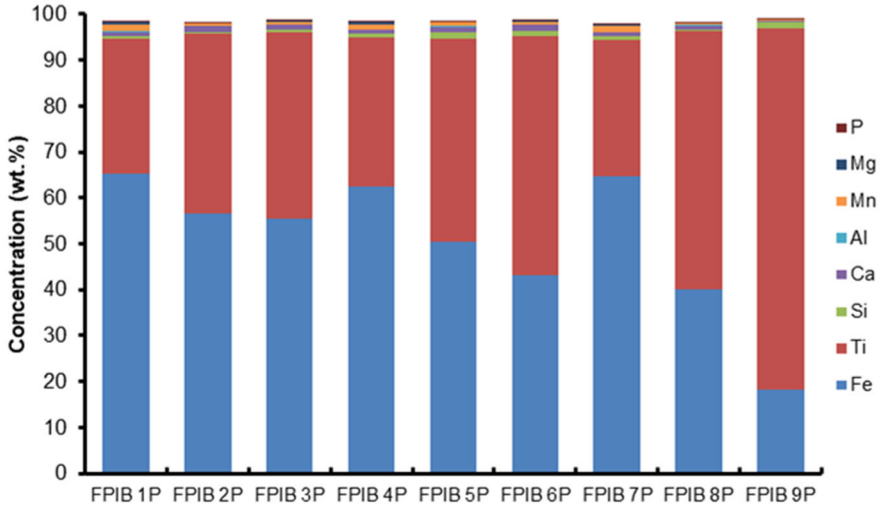

Fig 8. XRF analysis of the acid leaching residue

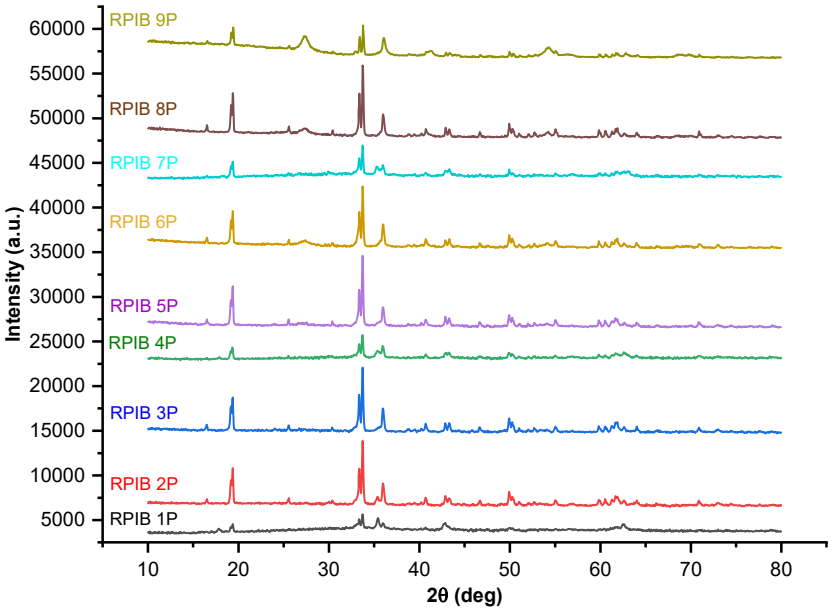

Fig 9. XRD pattern of the acid leaching residue

4P=RPIB 7P; RPIB 2P=RPIB 5P=RPIB 8P; and RPIB 3P=RPIB 6P=RPIB 9P). The identical XRD analysis results show that the HCl leaching process extracted titanium with nearly identical impurities while leaving the rest behind.

The effect of the HCl concentration is only visible in the peak intensity as measured by the XRD analysis. The intensity reading is proportional to the compound concentration in the acid leaching residue. The main mineral phases in the acid leaching residue, according to the XRD pattern, are calcium manganese titanium oxide ($Ca_4Mn_2O_{9.926}Ti$), calcium catena-divanadate (CaO_4V_2), chromium silicide ($CrSi_2$), and rutile (TiO_2).

■ CONCLUSION

Regression using RSM with a second-order polynomial equation model has an R^2 of 0.7938 and adjusted R^2 of 0.7408. Based on SCM, the rate of the leaching reaction of Ti from low-grade ilmenite is controlled by diffusion through the ash layer. The optimum operating conditions required are a temperature of 30 °C, a concentration of HCl 9 M, and a leaching time of 120 min.

■ NOTATION

t = leached Ti concentration, g/L
x_1 = leaching temperature, °C
x_2 = HCl concentration, M
x_3 = leaching time, minute
β = regression equation coefficient
T = temperature
C_{HCl} = HCl solution concentration
x = fraction mass of recovered Ti
k_f = first model reaction rate constant
k_d = second model reaction rate constant
k_r = third model reaction rate constant
RPIB 1P (T = 30 °C, C_{HCl} = 1M)
RPIB 2P (T = 30 °C, C_{HCl} = 5M)
RPIB 3P (T = 30 °C, C_{HCl} = 9M)
RPIB 4P (T = 60 °C, C_{HCl} = 1M)
RPIB 5P (T = 60 °C, C_{HCl} = 5M)
RPIB 6P (T = 60 °C, C_{HCl} = 9M)
RPIB 7P (T = 90 °C, C_{HCl} = 1M)
RPIB 8P (T = 90 °C, C_{HCl} = 5M)
RPIB 9P (T = 90 °C, C_{HCl} = 9M)

■ ACKNOWLEDGMENTS

We would like to thank the Research Center for Mining Technology-National Research and Innovation Agency (PRTPB-BRIN), Department of Chemical Engineering (Sustainable Mineral Processing Research Group), Faculty of Engineering, Universitas Gadjah

Mada for the facility and the financial support to complete this study.

CONFLICT OF INTEREST

The corresponding author states that there is no conflict of interest on behalf of all authors.

AUTHOR CONTRIBUTIONS

Yayat Iman Supriyatna: conceptualization, methodology, writing- reviewing and editing; Agus Prasetya: supervision, reviewing and editing; Himawan Tri Bayu Murti Petrus: supervision and methodology; Slamet Sumardi: data analysis; Widi Astuti: supervision; Priskila Natalia: investigation; Dicky Marsa Adythia: investigation.

REFERENCES

[1] Ministry of Energy and Mineral Resources (ESDM), 2022, *Neraca Sumber Daya Mineral, Batubara, dan Panas Bumi Indonesia Tahun 2021*, Geological Agency, Center for Mineral Resources, Coal and Geothermal, Bandung, Indonesia.

[2] U.S. Geological Survey, 2019, *Mineral Commodity Summaries 2019*, U.S. Geological Survey, Reston, VA, US, pp 204.

[3] U.S. Geological Survey, 2020, *Mineral Commodity Summaries 2020*, U.S. Geological Survey, Reston, VA, US, pp. 200.

[4] U.S. Geological Survey, 2021, *Mineral Commodity Summaries 2021*, U.S. Geological Survey, Reston, VA, US, pp. 200.

[5] U.S. Geological Survey, 2022, *Mineral Commodity Summaries 2022*, U.S. Geological Survey, Reston, VA, US, pp. 202.

[6] U.S. Geological Survey, 2023, *Mineral Commodity Summaries 2023*, U.S. Geological Survey, Reston, VA, US, pp. 210.

[7] Middlemas, S., Fang, Z.Z., and Fan, P., 2013, A new method for production of titanium dioxide pigment, *Hydrometallurgy*, 131-132, 107–113.

[8] Middlemas, S., Fang, Z.Z., and Fan, P., 2015, Life cycle assessment comparison of emerging and traditional titanium dioxide manufacturing processes, *J. Cleaner Prod.*, 89, 137–147.

[9] Gázquez, M.J., Bolívar, J.P., Garcia-Tenorio, R., and Vaca, F., 2014, A Review of the production cycle of titanium dioxide pigment, *Mater. Sci. Appl.*, 5 (7), 441–458.

[10] Guo, Y., Liu, S., Jiang, T., Qiu, G., and Chen, F., 2014, A process for producing synthetic rutile from Panzhihua titanium slag, *Hydrometallurgy*, 147-148, 134–141.

[11] Nguyen, T.T., Pham, K.N., Dinh, T.H., Tran, V.D.N., and Ullah, A., 2023, Preparation of TiO_2 pigment from ilmenite ore concentrate by molten alkaline process, *Vietnam J. Sci. Technol. Eng.*, 65 (2), 15–19.

[12] Gireesh, V.S., Vinod, V.P., Krishnan Nair, S., and Ninan, G., 2015, Catalytic leaching of ilmenite using hydrochloric acid: A kinetic approach, *Int. J. Miner. Process.*, 134, 36–40.

[13] Xiang, J., Pei, G., Lv, W., Liu, S., Lv, X., and Qiu, G., 2020, Preparation of synthetic rutile from reduced ilmenite through the aeration leaching process, *Chem. Eng. Process.*, 147, 107774.

[14] Wahyuningsih, S., Pramono, E., Firdiyono, F., Sulistiyono, E., Budi Rahardjo, S., Hidayattullah, H., and Anatolia, F.A., 2013, Decomposition of ilmenite in hydrochloric acid to obtain high grade titanium dioxide, *Asian J. Chem.*, 25 (12), 6791–6794.

[15] Haverkamp, R.G., Kruger, D., and Rajashekar, R., 2016, The digestion of New Zealand ilmenite by hydrochloric acid, *Hydrometallurgy*, 163, 198–203.

[16] Trujillo, D., and Managón, L., 2016, Titanium dioxide recovery from ilmenite contained in ferrotitaniferous sands from Mompiche-Ecuador, *J. Geol. Resour. Eng.*, 4, 175–183.

[17] Jabit, N.A, and Senanayake, G., 2018, Characterization and leaching kinetics of ilmenite in hydrochloric acid solution for titanium dioxide production, *J. Phys.: Conf. Ser.*, 1082 (1), 012089.

[18] Haverkamp, R.G., Wallwork, K.S., Waterland, M.R., Gu, Q., and Kimpto, J.A., 2022, Controlled hydrolysis of TiO_2 from HCl digestion liquors of ilmenite, *Ind. Eng. Chem. Res.*, 61 (19), 6333–6342.

[19] Aristanti, Y., Supriyatna, Y.I., Masduki, N.P., and Soepriyanto, S., 2018, Decomposition of Banten ilmenite by caustic fusion process for TiO_2

photocatalytic spplications, *IOP Conf. Ser.: Mater. Sci. Eng.*, 285 (1), 012005.

[20] Aristanti, Y., Supriyatna, Y.I., Masduki, N.P., and Soepriyanto, S., 2019, Effect of calcination temperature on the characteristics of TiO_2 synthesized from ilmenite and its applications for photocatalysis, *IOP Conf. Ser.: Mater. Sci. Eng.*, 478 (1), 012019.

[21] Supriyatna, Y.I., Sumardi, S., Astuti, W., Nainggolan, A.N., Ismail, A.W., Petrus, H.T.B.M., and Prasetya, A., 2020, Characterization and a preliminary study of TiO_2 synthesis from Lampung iron sand, *Key Eng. Mater.*, 849, 113–118.

[22] Supriyatna, Y.I., Astuti, W., Sumardi, S., Sudibyo, S., Prasetya, A., Ginting, L.I., Irmawati, Y., Asri, N.S., and Petrus, H.T.B.M., 2021, Correlation of nano titanium dioxide synthesis and the mineralogical characterization of ilmenite ore as raw material, *Int. J. Technol.*, 12 (4), 749–759.

[23] Hazan, R., Muhamad Yusop, M.A., Paulus, W., and Khaironie, M.T., 2020, Obtaining TiO_2 from ilmenite via alkaline fusion method, *Mater. Sci. Forum*, 1010, 385–390.

[24] Zhao, X., Yan, H., Yu, L., Tang, X., Liu, Z., Determination of high content of titanium in ilmenite by inductively coupled plasma-optical emission spectrometry with sodium peroxide alkali fusion, *Rock Miner. Anal.*, 39 (3), 459–466.

[25] Janssen, A., and Putnis, A., 2011, Processes of oxidation and HCl-leaching of Tellnes ilmenite, *Hydrometallurgy*, 109 (3-4), 194–201.

[26] Das, G.K., Pranolo, Y., Zhu, Z., and Cheng, C.Y., 2012, Leaching of ilmenite ores by acidic chloride solutions, *Hydrometallurgy*, 133, 94–99.

[27] Wanta, K.C., Tanujaya, F.H., Susanti, R.F., Petrus, H.T.B.M., Perdana, I., and Astuti, W., 2018, Studi kinetika proses atmospheric pressure acid leaching bijih laterit limonit menggunakan larutan asam nitrat konsentrasi rendah, *J. Rek. Pros.*, 12 (2), 77–384.

[28] Lienda Aliwarga, L., Reynard, R., and Victoria, A.V., 2019, Pengendapan titanium pada larutan pasir besi dalam asam sulfat, *Jurnal Teknologi Mineral dan Batubara*, 15 (2), 109–118.

[29] Liu, Y., Shao, D., Wang, W., Yi, L., Chen, D., Zhao, H., Wu, J., Qi, T., and Cao, C., 2016, Preparation of rutile TiO_2 by hydrolysis of $TiOCl_2$ solution: Experiment and theory, *RSC Adv.*, 6 (64), 59541–59549.

[30] Rahayuningsih, E., Subagya, I.S., Setiawan, F.A., and Petrus, H.T.B.M., 2019, Fresh neem leaves (*Azadirachta indica* A. Juss) extraction and application: An optimization using response surface methodology, *Asian J. Chem.*, 31 (11), 2567–2574.

[31] Craparo, R.M., 2007, "Significance Level" in *Encyclopedia of Measurement and Statistics 3*, Eds. Salkind, N.J., SAGE Publications, Thousand Oaks, CA, US, 889–891.

[32] Petrus, H.T.B.M., Wijaya, A., Iskandar, Y., Bratakusuma, D., Setiawan, H., Wiratni, W., and Astuti, W., 2018, Lanthanum and nickel recovery from spent catalyst using citric acid: quantitative performance assessment using response surface method, *Metalurgi*, 33 (2), 91–100.

[33] Huang, Z., 2017, Hydrolysis of Titanic Acid in Hydrochloric Acid Solution for Synthesis of TiO_2 Powder with Controlled Particle Size: Processes, Morphology, and Kinetic Study, *Thesis*, Department of Metallurgical Engineering, University of Utah, US.

[34] Zhang, Y., Fang, Z.Z., Xia, Y., Huang, Z., Lefler, H., Zhang, T., Sun, P., Free, M.L., and Guo, J., 2016, A novel chemical pathway for energy efficient production of Ti metal from upgraded titanium slag, *Chem. Eng. J.*, 286, 517–527.